Synthesis and biological evaluation of SANT-2 and analogues as inhibitors of the hedgehog signaling pathway

ARTICLE *in* BIOORGANIC & MEDICINAL CHEMISTRY · JULY 2009

Impact Factor: 2.79 · DOI: 10.1016/j.bmc.2009.06.008 · Source: PubMed

7 AUTHORS, INCLUDING:

Anita Büttner
National University of Singapore
15 PUBLICATIONS **180** CITATIONS
SEE PROFILE

Vasiliki Sarli
Aristotle University of Thessaloniki
39 PUBLICATIONS **560** CITATIONS
SEE PROFILE

Stefan Scholz
Helmholtz-Zentrum für Umweltforschung
72 PUBLICATIONS **1,681** CITATIONS
SEE PROFILE

Athanassios Giannis
University of Leipzig
222 PUBLICATIONS **4,588** CITATIONS
SEE PROFILE

Bioorganic & Medicinal Chemistry 17 (2009) 4943–4954

Contents lists available at ScienceDirect

Bioorganic & Medicinal Chemistry

journal homepage: www.elsevier.com/locate/bmc

Synthesis and biological evaluation of SANT-2 and analogues as inhibitors of the hedgehog signaling pathway

Anita Büttner [a,†], Katrin Seifert [a,†], Thomas Cottin [a], Vasiliki Sarli [a], Lito Tzagkaroulaki [a], Stefan Scholz [b], Athanassios Giannis [a,*]

[a] University of Leipzig, Institute for Organic Chemistry, Johannisallee 29, D-04103 Leipzig, Germany
[b] UFZ—Helmholz Centre for Environmental Research, Department of Cell Toxicology, Permoserstraße 15, 04318 Leipzig, Germany

ARTICLE INFO

Article history:
Received 3 April 2009
Revised 29 May 2009
Accepted 2 June 2009
Available online 10 June 2009

Keywords:
SANT-2
Cyclopamine
Hedgehog
Medaka
Cyclopia

ABSTRACT

Hedgehog (Hh) signaling plays an important role in cell signaling of embryonic development and adult tissue homeostasis. In vertebrates, the hh gene encodes three different unique proteins: sonic hedgehog (Shh), desert hedgehog (Dhh) and indian hedgehog (Ihh). Disruption of the Hh signaling pathway leads to severe disorders in the development of vertebrates whereas aberrant activation of the Hh pathway has been associated with several malignancies including Gorlin syndrome (a disorder predisposing to basal cell carcinoma, medulloblastoma and rhabdomyosarcoma), prostate, pancreatic and breast cancers. In vivo evidence suggests the antagonism of excessive Hh signaling provides a route to unique mechanism-based anti-cancer therapies. Recently the small molecule SANT-2 was identified as a potent antagonist of Hh-signaling pathway.

Here, we describe the synthesis, SAR studies as well as biological evaluation of SANT-2 and its analogues. Fifteen SANT-2 derivatives were synthesized and analyzed for their interference with the expression of the Hh target gene *Gli1* in a reporter gene assay. By comparison of structure and activity important molecular descriptors for *Gli* inhibition could be identified. Furthermore we identified derivative TC-132 that was slightly more potent than the parent compound SANT-2. Selected compounds were tested for Hh related teratogenic effects in the small teleost model medaka. Albeit Gli expression has indicated a 16-fold higher Hh-inhibiting activity than observed for the plant alkaloid cyclopamine, none of the tested compounds were able to induce the cyclopamine-specific phenotype in the medaka assay.

1. Introduction

The Hedgehog (Hh) signaling pathway regulates numerous processes involved in patterning, proliferation, survival and growth in embryonic development as well as in adult tissue homeostasis.[1] In mammals, three Hedgehog genes, Sonic (Shh) Indian (Ihh) and Desert (Dhh) expressed specifically in different cell types are known. After their biosynthesis they are post-translationally modified with a palmitoyl group at their N-terminal cystein residue and with a cholesterol moiety at their C-terminal glycin residue.[2] Hh proteins are secreted lipidated proteins that bind 12 pass transmembrane receptors Patched1 (Ptch1) and Ptch2. They are binding to these receptors induces internalisation of Patch and derepression of the activity of Smoothened (Smo), a 7 pass transmembrane receptor. After binding of Hh to Ptch, Smo is phosphorylated[3] and translocated from endosomes to the tip of the cilium resulting in the inhibition of processing of transcription factors *Gli1/2*.[4] Inappropriate Shh signaling has been associated with several malignancies including Gorlin syndrome (an autosomal dominant inherited disorder predisposing to basal cell carcinoma, medulloblastoma and rhabdomyosarcoma) as well as tumors of the gastrointestinal tract, small cell lung cancers, pancreatic carcinomas and prostate cancers.[5–8]

Antagonism of excessive Hh signaling may provide a route to unique mechanism-based anti-cancer therapies. Therefore small molecules inhibitors of Hh signaling are of great therapeutic potential.[9] Recently, a number of small molecules that act as Shh antagonists have been reported both in scientific and patent literature. They include the steroidal alkaloid cyclopamine,[10] biarylcarboxamides,[11] CUR61414,[12] SANT1-4,[13,14] JK184,[15] and GANT61.[16] Furthermore, important insights into the mechanism of action of some of these inhibitors were published.[17] For example it was shown that cyclopamine drives Smo to the primary cilium were it is inhibited by this alkaloid. Conversely, other antagonists including SANT-2 and GANT61 abrogate the Shh-dependent translocation of Smo to the primary cilium.

* Corresponding author. Fax: +49 341 9736599.
E-mail address: giannis@uni-leipzig.de (A. Giannis).
† These authors contributed equally to this work.

0968-0896/$ - see front matter © 2009 Elsevier Ltd. All rights reserved.
doi:10.1016/j.bmc.2009.06.008

SANT-2, a member of the benzimidazole class of compounds, is a very potent inhibitor of hedgehog signaling effective in nanomolar concentrations by inhibiting both wild type and oncogenic Smo.[13]

The aim of this study was to establish a synthetic route to SANT-2 and its analogues in order to evaluate their potential inhibitory effects on the hedgehog pathway. Furthermore we wanted to perform some SAR studies using these analogues. We modified SANT-2 at its benzimidazole moiety and altered the pattern of substitution particularly at the phenyl ring. Shh inhibition was measured by analyzing the expression of the hedgehog target transcription factor gene *Gli1* in a reporter gene assay. Furthermore, teratogenic effects were analyzed in the small model teleost medaka (*Oryzias latipes*) for selected compounds. Shh-antagonists such as the plant alkaloid cyclopamine are known to induce the cyclopia phenotype in vertebrates. For teleosts this phenotype has been described in zebrafish and medaka[18] with more severe manifestation in the medaka. Cyclopia[19] or hosoprosencephaly is a disorder that is characterized by failure of the embryo's forebrain to divide and to form a bilateral hemisphere during development. Exposure of medaka embryos was performed in order to identify Shh-associated or other potential non-Shh related teratogenic effects. These disorders may be important indicators for side effects in preclinical studies.

2. Results and discussion

2.1. Synthesis of SANT-2 and analogues

Commercially available benzene-1,2-diamine reacted with 2-chloro-5-nitrobenzoyl chloride and yielded amide **3** which was subsequently cyclised to benzimidazole **4** under acidic conditions.[20] Reduction of the nitro group in the presence of iron powder, HCl and EtOH afforded aniline **5**, which was further used for N-acylation reactions, Figure 1. Additionally, we synthesized benzoxazole, benzothiazole, imidazole, and indole derivatives as SANT-2 analogues as depicted in Figures 2 and 3.

2.2. Inhibition of *Gli1* reporter gene expression

The different derivatives were tested for their interference with the Shh signaling pathway by an established reporter gene assay based on the inhibition of the target gene *Gli1*. The IC_{50}-values and their corresponding confidence intervals for inhibition of the *Gli1* reporter gene were determined (Table 1, Fig. 4A). Compounds with non-overlapping confidence intervals were considered to exhibit significantly different IC_{50} values. According to the IC_{50}-values and their confidence intervals the derivatives could be classified into four different groups (Fig. 4B–E). Group 1 (Fig. 4B) had similar IC_{50}-values as the parent compound SANT-2. Group 2 (Fig. 4C) had approximately twofold higher IC_{50} values. About 10-fold higher IC_{50}-values were observed for group 3 (Fig. 4D). No activity at all could be detected for compounds summarised in group 4 (Fig. 4E). Analysis of the molecular structure revealed striking similarities for most of the compounds within one of the groups. Group 1 comprised chemicals with modifications exclusively at the western aryl moiety. With the exception of compound KS-B all members of this group had at least one ethoxy or methoxy substitution at position 3 of the phenyl ring. Compounds summarised in group 2 were characterised by the absence of ethoxy and methoxy substitution in positions 3, 4 and 5 of the phenyl ring and/or the presence of a cyano, dimethylamino, chloride or fluoride substitution in position 3 of the *N*-phenyl ring. Compounds with an additional methoxy group at position 2 of the phenyl ring or removal of the Cl-substitution at the benzimidazole formed group 3 of SANT-derivatives. Group 4 comprised compounds with substitutions within the benzimidazole ring. The data clearly show that the benzimidazole core is essential for inhibitory properties. Minor effects are obtained by changes at the benzoic acid moiety. One derivative (TC132) was shown to be slightly more potent than the parent compound SANT-2. Similar observations were made for a structurally related group of compounds, that is, JRK184 and its derivatives.[15] In JRK184 derivatives the imidazopyridine core—the analogous moiety to the benzimidazole core in SANT-derivatives—is essential for inhibition of *Gli1*. Substitutions of the phenyl ring were of minor relevance. TC132, the compound with the highest efficacy in the present study, exhibited an IC_{50} of 80 nM. Some JRK derivates showed a slightly higher activity with IC_{50} values of about 30 nM. Both studies show that the identification of molecular descriptors important for Shh inactivation—measured by *Gli1*-inhibition—provides a possibility for the generation of further derivatives with higher bioactivity.

2.3. Induction of cyclopia phenotype in the medaka

Compounds interfering with the Shh signaling pathway, such as the Smo binding alkaloid cyclopamine can induce the cyclopia phenotype in vertebrates. This phenotype, which is characterized by one fusion eye, has been observed in mammals and birds[21] and in a less severe form also for the small teleost medaka. The medaka offers the opportunity to screen for Shh-related teratogenic effects by screening for the cyclopia phenotype in a small-scale system.

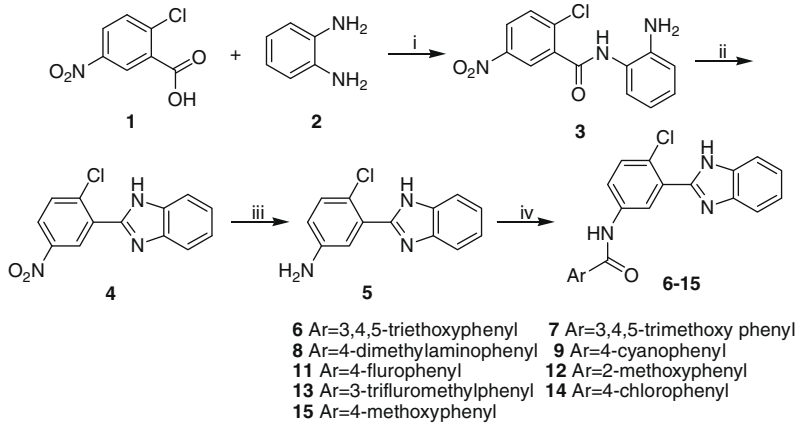

Figure 1. Reagents and conditions: (i) (a) $(COCl)_2$, DMF cat., CH_2Cl_2, rt 2 h; (b) Et_3N, THF, rt, 12 h; (ii) CH_3COOH, reflux, 2 h; (iii) Fe, HCl, EtOH, reflux, 2 h; (iv) (a) ArCOOH, $(COCl)_2$, DMF cat., CH_2Cl_2, rt 2.5 h; (b) Et_3N, THF, rt, 2.5 h.

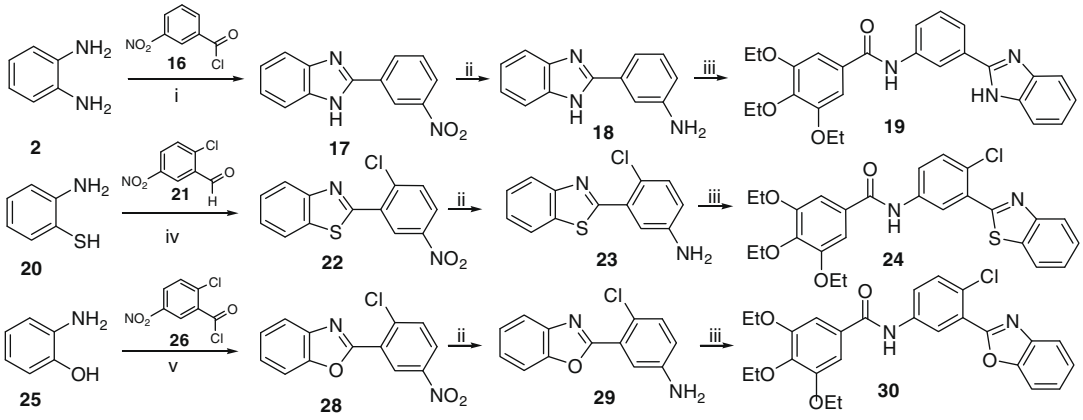

Figure 2. Reagents and conditions: (i) (a) Et_3N, THF, rt, 12 h; (b) CH_3COOH, reflux, 2 h; (ii) Fe, HCl, EtOH, reflux, 2–3 h; (iii) 3,4,5-triethoxybenzoyl chloride, Et_3N, DMAP, THF, rt 15–36 h; (iv) I_2, DMF, rt 15 h; (v) (a) Et_3N, THF, rt, 15 h; (b) *p*-TsOH, xylole, reflux, 4 h.

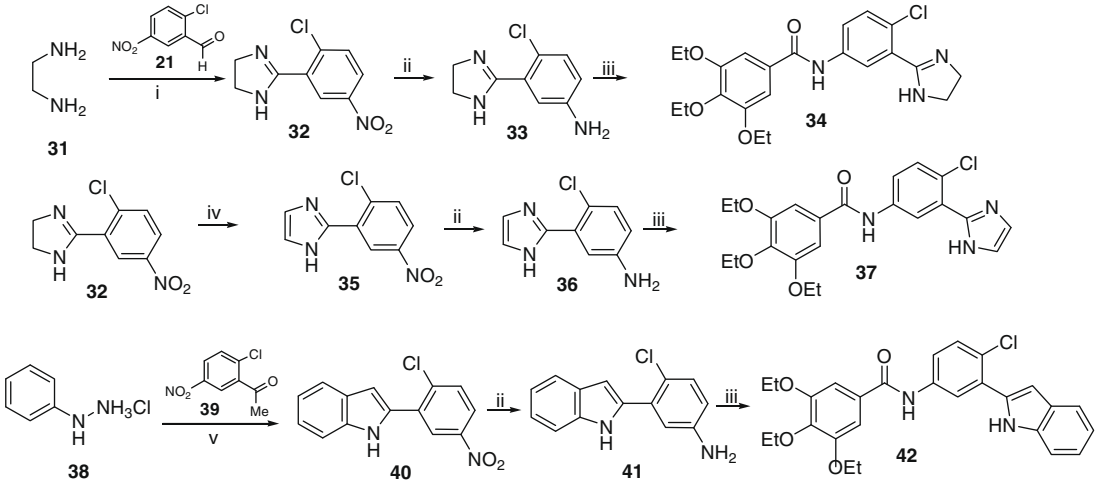

Figure 3. Reagents and conditions: (i) (a) I_2, K_2CO_3, *t*-BuOH, 70 °C, 3 h; (ii) Fe, HCl, EtOH, reflux, 2–3 h; (iii) (a) 3,4,5-triethoxybenzoic acid, $(COCl)_2$, DMF cat.; (b) Et_3N, CH_2Cl_2, rt, 12 h; (iv) DIB, K_2CO_3, DMSO, rt 3d; (v) (a) AcOH, EtOH, 80 °C, 12 h; (b) PPA, 120 °C, 15 min.

Table 1
IC_{50}-values, slope (*p*) of non-linear regression curves (Hill-slope equation), corresponding standard errors (SE) and confidence intervals for the inhibition of *Gli1* reporter gene expression in Shh-Light II cells by SANT-2 and its derivatives (see also Fig. 4 for graphical representation and compound structures)

Compound	No.	IC_{50} (nM)	SE	Confidence interval		Slope (*p*)	SE
				Lower level	Upper level		
TC132	7	79.8	7.9	65	98	1.3	0.18
SANT-2	6	97.9	8.9	81	118	1.1	0.10
KSA	15	117	9.7	99	140	1.3	0.12
KSB	13	119	13	96	145	1.1	0.12
TC135	10	163	16	133	201	1.1	0.10
TC134	9	185	23	144	239	1.6	0.21
TC133	8	190	29	140	259	0.8	0.09
KSC	14	224	27	174	287	1.2	0.13
TC136	11	251	23	209	301	1.3	0.11
TC137	12	876	94	702	1207	1.4	0.23
TC145	18	1325	603	647	3653	0.64	0.19
Cyclopamine		1312	95	1246	1593	2.11	0.37
TC146	23	n.d.	–	–	–	–	–
TC147	28	n.d.	–	–	–	–	–
KS79	32	n.d.	–	–	–	–	–
KS80	35	n.d.	–	–	–	–	–
KS83	40	n.d.	–	–	–	–	–

Cyclopamine was included for comparison and as well-known Shh inhibiting reference compound. *Gli1* expression was measured in shh light II cells co-treated with the hedgehog activator SAG. IC_{50} values were calculated from 4 replicated independent experiments except TC137 ($N = 3$), TC145 ($N = 2$) and cyclopamine ($N = 2$). n.d. = no effect detected within the tested range of concentrations. Highest tested concentration of each compound = 5000 nM. Numbers in column 2 refer to numbers given in the description for the chemical synthesis.

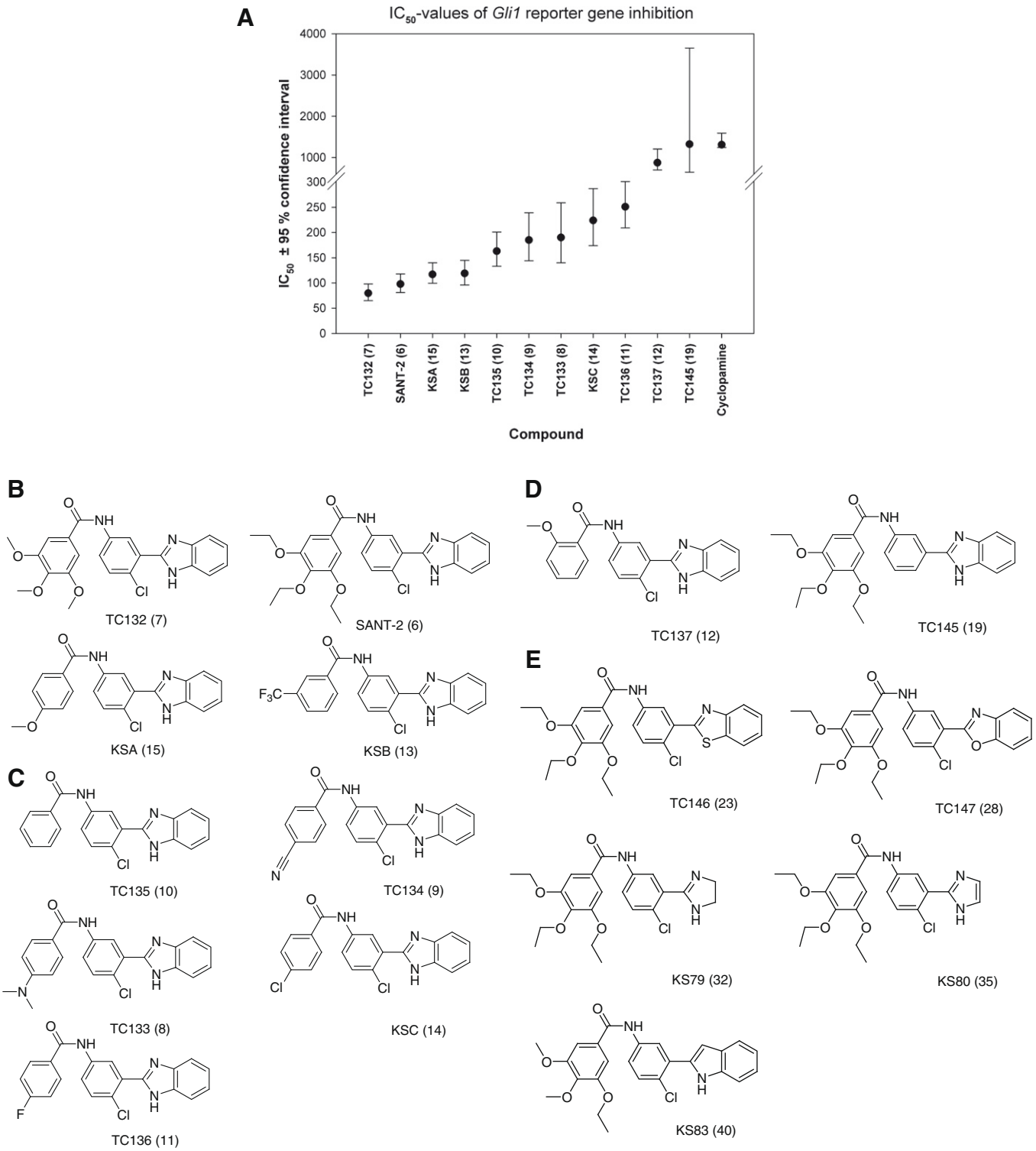

Figure 4. (A) IC_{50}-values (in nM) for the inhibition of *Gli1* reporter gene expression in Shh- Light II cell exposed to 100 nM SAG and various concentrations of SANT-2 and its derivatives. Cyclopamine was included for comparison and as well-known Shh inhibiting reference compound. Data points represent IC_{50}-values ± upper and lower confidence interval. Each compound was tested in four independent experiments, except TC137 ($N = 3$), TC145 ($N = 2$) and cyclopamine ($N = 2$). Numbers in brackets refer to numbers given in the description for the chemical synthesis. (B–E) Structures of SANT-2 derivatives grouped according to their efficacy in inhibiting *Gli1* reporter gene expression (see Section 2 for further details).

Other teratogenic effects or unknown bioactivities of the test compound may be detected as well. In contrast to the cellular screening system based on *Gli1* expression, it provides the advantage to represent a complex system based on a complete organism. In the present study, SANT-2 and two of the most potent *Gli1*-inhibiting derivatives (TC132, KSB) identified from the *Gli1*-reporter gene assay, were also analyzed for their effects on medaka development.

Cyclopamine was used as reference compound. It provokes the cyclopia phenotype in concentrations of about 10-fold (12.5 μM) above the IC_{50}-values (1.3 μM) of *Gli1*-reporter gene expression.

The tested compounds were 11–16-fold more potent inhibitors of *Gli1* expression if compared to cyclopamine. However, none of them induced the cyclopia phenotype in the tested range of concentrations (0.01–100 μM). At concentrations close to lethality (10–50 μM), in the range of concentrations for cyclopamine-induced cyclopia, a strong delay in development was observed indicating toxic effects (Fig. 5). The failure to induce the cyclopia phenotype in the embryo is conflicting, as strong inhibitors of *Gli1* expression should be expected to induce this phenotype as well. The relatively weak sensitivity of the medaka embryo assay (ca. 10-fold less if compared to the IC_{50}-values of cyclopamine) does not explain this failure. Based on the IC_{50}-values of the *Gli1* reporter gene assay, induction of the cyclopia phenotype by SANT-2 derivatives should have been expected in the range of 100–1000 nM. Differences in the uptake and distribution of cyclopamine and SANT-2 derivatives or reduced bioavailability due to storage in the lipophilic yolk may have caused the failure to induce cyclopia. However, injection of SANT-2 at the 1-cell stage into the cytoplasm, the yolk or the perivitellin space did not cause cyclopia as well (data not shown). Alternatively, additional unknown bioactivities of SANT-2 and its derivatives that are not detected by the reporter gene assay may overlap Shh inhibition and prevent the manifestation of the cyclopia phenotype. Finally the different mechanism of action of cyclopamine and SANT-2 (vide supra) should be taken into consideration.

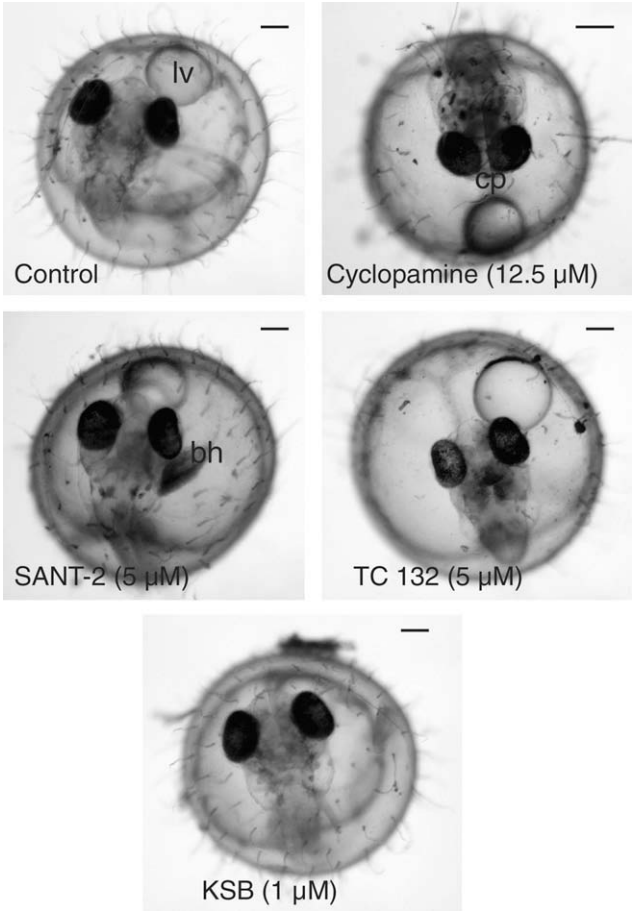

Figure 5. Development of medaka embryos exposed to potential Shh inhibiting compounds. Exposure to the Shh reference inhibitor cyclopamine induced the cyclopia phenotype (indicated by a reduced distance of the eyes, cp). SANT-2 and its derivatives did not induce cyclopia but provoked developmental delays shown by smaller and less pigmented eyes. Blood hemorrhagia (bh) was also observed in some cases. All images were recorded at 5 days post fertilization and are representative examples of 15 embryos exposed per compound and concentrations. The scale bar represents 100 μm.

2.4. Conclusions

We have shown that modifications of aryl moieties and particularly the benzimidazole core in SANT-2 reduce the ability of

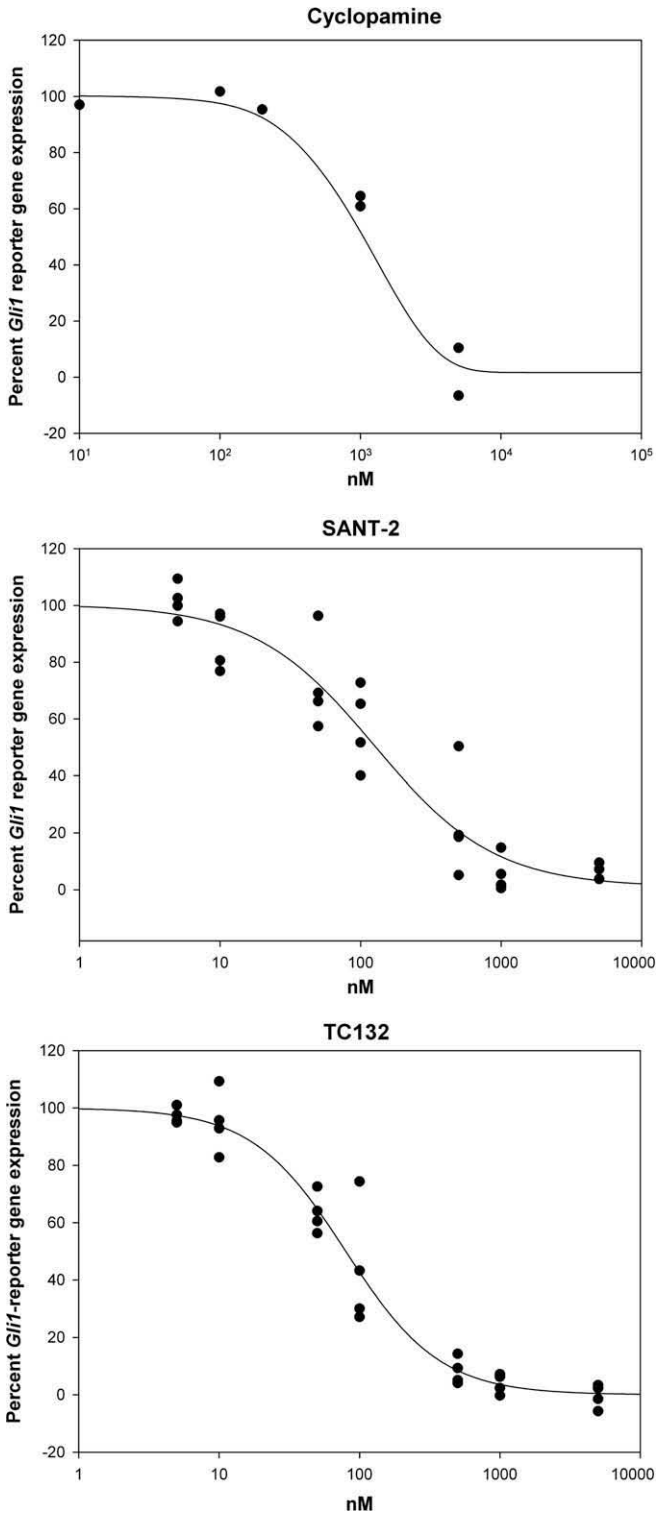

Figure 6. Examples of concentration–response curves for cyclopamine ($N = 2$), SANT-2 ($N = 4$) and the SANT-2 derivative TC132 ($N = 4$). Numbers refer to independent experiments.

derivatives to inhibit the Shh signaling pathway. The chlorine substituent in SANT-2 is also important for activity. Exposure of medaka embryos to SANT-2 and derivatives did not provoke the cyclopia phenotype, although this effect could have been expected based on the inhibition of *Gli1* expression relative to the inhibition by cyclopamine. The analysis of *Gli1*-inhibition and phenotypic effects represent a powerful combination to identify potential Shh-inhibitors and the molecular descriptors of their biological activity. Both assays provide an efficient way to identify potential drug candidate compounds for the treatment of Shh-associated cancers. While screening of G*li1*-expression is principally able to identify Shh antagonists, the embryo assay can be used to identify teratogenic, toxic and unwanted side effects in a complex system and limit the number of compounds subjected to further analysis.

3. Experimental

3.1. Biological tests

Cell assay inhibition of *Gli1*-expression was measured in Shh-Light II cells (ATCC CRL-2795, LGC, Wesel, Germany) co-exposed to 100 nM of the Hh agonist SAG as described by Beachy et al.[9] Stock solutions of the potential inhibitors of Hh were prepared in ethanol and introduced in different concentration into the culture medium to reach a final solvent concentration of 0.1%. After treatment for 48 h cells were washed with PBS. Harvest and lysis of the cells, measurement of reporter gene and constitutive *Renilla* luminescence were performed with the Dual Luciferase® reporter gene system according to the manufacturer's instructions (Promega, Mannheim, Germany). Luminescence was recorded by using a GENios reader (TECAN, Crailsheim, Germany). For determination of IC_{50} values, the relative luminescence units per second RLU/s (quotient of firefly and renilla luminescence) were plotted against the inhibitor concentrations. Each assay was replicated at two to four times (independent experiments) with three technical replicates each.

Analysis of constitutive *Renilla* luminescence was used to normalise for any potential unspecific inhibition of *Gli1*-reporter gene luminescence. Furthermore, microscopic observations of cells did not indicate any toxic effects up to a concentration of 5 μM, the highest concentration tested for all compounds.

Medaka cyclopia assay Medaka of the CAB strain (kindly provided by Professor J. Wittbrodt, EMBL, Heidelberg, Germany) were cultured at 26 °C and a light cycle of 14:10 h light/dark. For breeding, one female and one male were placed in 3 L tanks in a circulation system. Eggs were collected within 1–2 h after fertilization by removing them from the female's belly. Fertilized eggs were exposed to different inhibitor concentrations in local tap water (pH 8–8.2, water hardness 1.2–2.4 mM bivalent ions, conductivity 520e560 mS/cm) supplemented with 0.1% methylene blue. Compounds were added by stock solutions in ethanol with final solvent concentrations of 1%. Controls were treated with 1% ethanol only. Exposure started at 4–5 hpf and was continued until 5 days post fertilisation at 26 °C. Embryos were visually inspected for the cyclopia phenotype (reduced eye distance). Images were recorded with a digital consumer camera attached to a dissection microscope (MZ 16F, Leica, Wetzlar, Germany).

3.2. Statistical analysis

Concentration–response curves of *Gli1*-reporter gene luminescence were fitted with the Hill-slope equation:

$$y = \mathrm{Min} + \frac{\mathrm{Max} - \mathrm{Min}}{1 + \left(\frac{x}{IC_{50}}\right)^{-p}}$$

Data were first normalised so that individual dose–response curves converged to 0 and 100. Subsequently, these normalised data were used to calculate the IC_{50} and corresponding SE and confidence intervals based on 2–4 replicates. Examples for the calculation of concentration–response curves are shown for cyclopamine, SANT-2 and TC132 in Figure 6. Calculations were performed using the software jmp (SAS Institute Inc., Cary, NC). IC_{50} with non-overlapping confidence intervals ($p < 0.05$) were considered as significantly different.

4. Chemistry

4.1. General

All materials were obtained from commercial suppliers and used without further purification. All anhydrous reactions were performed under argon atmosphere. All reactions were monitored by TLC (silica gel, GF_{254}) with UV light and ninhydrin visualization. Flash chromatography was performed on Merck Silica Gel 60. Melting points were uncorrected and were determined on a Büchi Melting Point B-540 apparatus. ^1H and ^{13}C NMR spectra were recorded on Varian Gemini 2000, Varian Mercury plus 300 and Varian Mercury plus 400 NMR spectrometers at room temperature. High-resolution (HR) mass spectra were obtained with a 7 T APEX II mass spectrometer. Yields are not optimised.

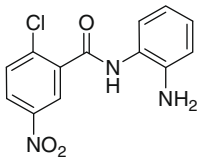

4.1.1. *N*-(2-Aminophenyl)-2-chloro-5-nitrobenzamide (3)

To a solution of 2-chloro-5-nitrobenzoic acid **1** (4.03 g, 19.99 mmol) in dry CH_2Cl_2 (20 ml) was added oxalylchloride (1.80 ml, 20.99 mmol), followed by two drops of DMF at 0 °C under argon atmosphere. The resulting mixture was stirred at 0 °C for 30 min and then 1.5 h at room temperature. The solvent was evaporated in vacuo to give a yellow solid. The crude acyl chloride (1.1 equiv) was added into an ice-cooled solution of 1,2-diaminobenzene **2** (2.12 g, 19.60 mmol) and Et_3N (4.13 ml, 29.40 mmol) in anhydrous THF (80 ml). After stirring over night at room temperature the volatiles were removed under reduced pressure, and the residue was purified by silica gel FC (EtOAc/hexane, 3:2, *v*/*v*) to obtain **3** as a yellow solid (3.89 g, 68%); mp = 170–171 °C; ^1H NMR (300 MHz, $(CD_3)_2SO$): δ = 5.00 (s, 2H), 6.58 (dt, *J* = 7.5 Hz, 1.5 Hz, 1H), 6.76 (dd, *J* = 7.8 Hz, 1.5 Hz, 1H), 6.98 (dt, *J* = 7.8 Hz, 1.5 Hz, 1H), 7.26 (dd, *J* = 7.8 Hz, 1.5 Hz, 1H), 7.85 (d, *J* = 8.7 Hz), 8.30 (dd, *J* = 8.7 Hz, 2.7 Hz, 1H), 8.59 (d, *J* = 2.7 Hz, 1H), 9.89 (s, 1H); ^{13}C NMR (75 MHz, $(CD_3)_2SO$): δ = 115.8, 116.0, 121.9, 124.1, 125.4, 126.2, 126.9, 131.1, 137.2, 138.0, 142.9, 146.1, 163.2; ESI-HRMS *m*/*z* calcd for $C_{13}H_{10}ClN_3O_3$: 314.03029 [M+Na$^+$], found: 314.02021.

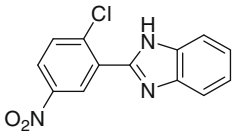

4.1.2. 2-(2-Chloro-5-nitrophenyl)-1*H*-benzo[*d*]imidazole (4)

N-(2-Aminophenyl)-2-chloro-5-nitrobenzamide **3** (3.58 g, 12.26 mmol) was dissolved in glacial AcOH (130 ml) and refluxed for 2 h. After treatment with ice-water (190 ml) the obtained precipitate was washed with a small among of ice water. Again,

the filtrate was treated with ice (200 g) and after filtration the combined precipitates were washed with a small among of ether and dried over night. The crude material was purified by FC (hexane/EtOAc, 2:1 *v*/*v*, then gradient of hexane/acetone, 4:1–0:1, *v*/*v*) and gave **4** as a yellow solid (2.71 g, 81%); mp = 198–199 °C; ^{1}H NMR (300 MHz, $(CD_3)_2SO$): δ = 7.23 (dd, *J* = 6.0 Hz, 3.3 Hz, 2H), 7.65 (dd, *J* = 6.0 Hz, 3.3 Hz, 2H), 7.90 (d, *J* = 8.7 Hz, 1H), 8.28 (dd, *J* = 8.7 Hz, 3.0 Hz, 1H), 8.74 (d, *J* = 2.7 Hz, 1H); ^{13}C NMR (100 MHz, $(CD_3)_2SO$): δ = 115.8, 122.4, 125.0, 126.4, 131.2, 132.1, 138.1, 139.4, 146.3, 147,6; ESI-HRMS *m/z* calcd for $C_{13}H_8ClN_3O_2$: 569.05023 [2M+Na$^+$], found: 569.05028.

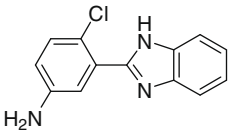

4.1.3. 3-(1*H*-Benzo[*d*]imidazol-2-yl)-4-chloroaniline (5)

To a solution of 2-(2-chloro-5-nitrophenyl)-1*H*-benzimidazole **4** (2.40 g, 8.77 mmol) in ethanol (31 ml) was added iron powder (1.47 g, 26.28 mmol) and concd HCl (3.7 ml). The mixture was heated to reflux under argon for 2 h. The cooled solution was diluted with EtOAc (120 ml) and water (120 ml), and the layers were separated. The aqueous layer was washed with EtOAc (120 ml) three times. The combined organic layers were filtered through Celite, washing with water (100 ml) and satd K_2CO_3 solution (100 ml) and dried over Na_2SO_4. The solvent was removed under reduced pressure and the residue was purified by column chromatography using EtOAc as eluent to furnish **5** as a brown solid (1.62 g, 76%); mp = 209–210 °C; ^{1}H NMR (300 MHz, $(CD_3)_2SO$): δ = 5.47 (s, 2H), 6.69 (dd, *J* = 8.7 Hz, 3.0 Hz, 1H); 7.11 (d, *J* = 3.0 Hz, 1H), 7.19–7.22 (m, 3H), 7.54–7.63 (m, 2H), 12.50 (s, 1H); ^{13}C NMR (50 MHz, $(CD_3)_2SO$): δ = 115.4, 116.4, 116.6, 116.9, 122.0, 129.9, 130.5, 147.9, 149.9; ESI-HRMS *m/z* calcd for $C_{13}H_{10}ClN_3$: 244.06360 [M+H$^+$], found: 244.06357.

4.2. General procedure for preparing benzimidazoles 6–15

Substituted benzoic acids (4.01 mmol) were dissolved in dry CH_2Cl_2 (4 ml) and cooled to 0 °C under argon. Oxalylchloride (0.4 ml, 4.21 mmol) and two drops of DMF were added and the resulting mixture was stirred at 0 °C for 1.5 h and then 1 h at room temperature. The solvent was evaporated in vacuo to give a solid that was dried in vacuo. Part of the obtained crude acyl chloride (1.73 mmol, 1.05 equiv) was dissolved in THF (5 ml), and added drop wise into an ice-cooled solution of the corresponding aniline of type **5** (1.64 mmol) and Et_3N (2.46 mmol) in anhydrous THF (5 ml). After stirring an additional 1 h at 0 °C and 2.5 h at room temperature the solvent was removed under reduced pressure, and the residue was chromatographed on silica gel to obtain the corresponding anilides.

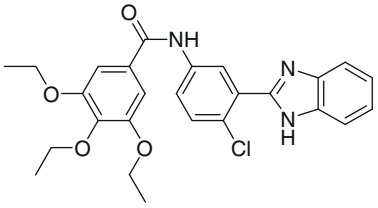

4.2.1. *N*-(3-(1*H*-Benzo[*d*]imidazol-2-yl)-4-chlorophenyl)-3,4,5-triethoxybenzamide (6, SANT-2)

SANT-2 was obtained as a white solid in 80% yield from 3,4,5-triethoxybenzoic acid. Mp = 210–211 °C; ^{1}H NMR (300 MHz, $(CD_3)_2SO$): δ = 1.24 (t, *J* = 7.1 Hz, 3H), 1.35 (t, *J* = 6.9 Hz, 6H), 4.01 (q, *J* = 7.0 Hz, 2H), 4.10 (q, *J* = 7.1 Hz, 4H), 7.22–7.29 (m, 4H), 7.61–7.64 (m, 3H), 8.02 (dd, *J* = 8.7 Hz, 2.7 Hz, 1H), 8.38 (d, *J* = 2.7 Hz, 1H), 10.33 (br, 1H), 12.69 (br, 1H); ^{13}C NMR (50 MHz, $(CD_3)_2SO$): δ = 15.4, 16.2, 65.0, 68.8, 107.1, 112.6, 122.5 123.4, 124.3, 126.1, 129.8, 130.6, 131.2, 139.1, 140.9, 143.8, 149.6, 152.9, 165.7; ESI-HRMS *m/z* calcd for $C_{26}H_{27}ClN_3O_4$: 480.16901 [M+H$^+$], found: 480.16825.

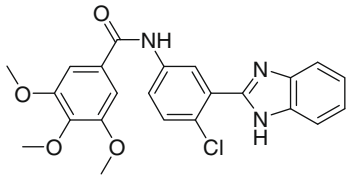

4.2.2. *N*-(3-(1*H*-Benzo[*d*]imidazol-2-yl)-4-chlorophenyl)-3,4,5-trimethoxybenzamide (7, TC-132)

White solid, yield 41%. Mp = 257–258 °C; ^{1}H NMR (300 MHz, $(CD_3)_2SO$): δ = 3.73 (s, 3H), 3.87 (s, 6H), 7.22–7.25 (m, 2H), 7.32 (s, 2H), 7.62–7.65 (m, 3H), 8.03 (dd, *J* = 8.7 Hz, 2.7 Hz, 1H), 8.38 (d, *J* = 2.7 Hz, 1H), 10.38 (s,1H), 12.69 (s, 1H); ^{13}C NMR (75 MHz, $(CD_3)_2SO$): δ = 56.1, 60.1, 105.4, 122.7, 123.6, 125.4, 129.4, 129.8, 130.6, 138.3, 140.6, 148.9, 152.7, 165.0; ESI-HRMS *m/z* calcd for $C_{23}H_{20}ClN_3O_4$: 438.12151 [M+H$^+$], found: 438.12149.

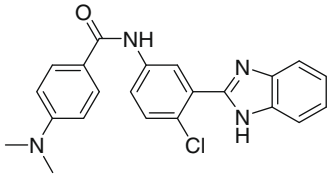

4.2.3. *N*-(3-(1*H*-Benzo[*d*]imidazol-2-yl)-4-chlorophenyl)-4-(dimethylamino)benzamide (8)

Orange solid, yield 90%. Mp = 208–215 °C; ^{1}H NMR (200 MHz, $(CD_3)_2SO$): δ = 2.96 (br, 6H), 6.73 (d, *J* = 9.2 Hz, 2H), 7.19–7.24 (m, 2H), 7.54–7.62 (m, 2H), 7.79–7.90 (m, 3H), 7.99 (dd, *J* = 9.2 Hz, 2.6 Hz, 1H), 8.40 (d, *J* = 2.6 Hz, 1H), 10.14 (s, 1H); ^{13}C NMR (50 MHz, $(CD_3)_2SO$): δ = 40.3, 111.4, 111.8, 121.1, 123.0, 123.8, 125.4, 129.9, 130.5, 131.1, 132.7, 139.7, 149.8, 153.2, 154.8, 166.0; ESI-HRMS *m/z* calcd for $C_{22}H_{19}ClN_4O$: 391.13202 [M+H$^+$], found: 391.13209.

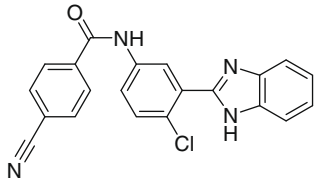

4.2.4. *N*-(3-(1*H*-Benzo[*d*]imidazol-2-yl)-4-chlorophenyl)-4-cyanobenzamide (9)

Red solid, yield 61%. Mp = 225–227 °C; ^{1}H NMR (400 MHz, $(CD_3)_2SO$): δ = 7.25 (d, *J* = 4.8 Hz, 2H), 7.61–7.71 (m, 3H), 8.00 (dd, *J* = 8.4 Hz, 2.8 Hz, 1H), 8.04 (d, *J* = 8.4 Hz, 2H), 8.15 (d, *J* = 8.4 Hz, 2H), 8.45 (d, *J* = 2.8 Hz, 1H), 10.77 (s, 1H), 12.72 (s, 1H); ^{13}C NMR (100 MHz, $(CD_3)_2SO$): δ = 111.9, 114.1, 118.3, 119.0, 121.8, 122.7, 122.8, 123.5, 125.9, 128.6, 130.0, 130.7, 132.5, 134.8, 138.0, 138.4, 143.1 148.9, 164.3; ESI-HRMS *m/z* calcd for $C_{21}H_{13}ClN_4O$: 373.08507 [M+H$^+$], found: 373.08512.

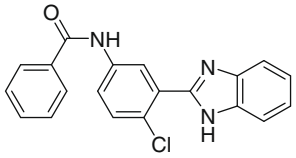

4.2.5. *N*-(3-(1*H*-Benzo[*d*]imidazol-2-yl)-4-chlorophenyl)-benzamide (10)

White solid, yield 58%. Mp = 272 °C; ^{1}H NMR (200 MHz, $(CD_3)_2SO$): δ = 7.20–7.24 (m, 2H), 7.48–7.63 (m, 6H), 8.0 (dd, *J* = 7.8 Hz, 1.6 Hz, 3H), 8.44 (d, *J* = 2.8 Hz, 1H), 10.53 (s, 1H), 12.70 (s, 1H); ^{13}C NMR (75 MHz, $(CD_3)_2SO$): δ = 111.8, 119.0, 121.9, 122.6, 123.4, 125.5, 127.7, 128.4, 129.9, 130.5, 131.8, 134.4, 138.4, 143.0, 149.0, 165.7; ESI-HRMS *m/z* calcd for $C_{20}H_{14}ClN_3O$: 348.08982 [M+H$^+$], found: 348.08987.

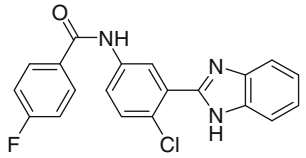

4.2.6. *N*-(3-(1*H*-Benzo[*d*]imidazol-2-yl)-4-chlorophenyl)-4-fluorobenzamide (11)

White solid, yield 94%. Mp = 241 °C; ^{1}H NMR (300 MHz, $(CD_3)_2SO$): δ = 7.23–7.24 (m, 2H), 7.37 (t, *J* = 8.7 Hz, 2H), 7.58–7.63 (m, 2H), 7.70 (d, *J* = 6.6 Hz, 1H), 7.99 (dd, *J* = 8.7 Hz, 2.4 Hz, 1H), 8.08 (dd, *J* = 8.7 Hz, 5.7 Hz, 2H), 8.44 (d, *J* = 2.4 Hz, 1H), 10.55 (s, 1H), 12.70 (s, 1H); ^{13}C NMR (100 MHz, $(CD_3)_2SO$): δ = 115.3, 115.5, 111.8/119.0 (d, *J* = 720 Hz), 121.8, 122.6, 122.8, 123.4, 125.5, 129.9, 130.4, 130.5/130.6 (d, *J* = 1.5 Hz), 130.8/130.9 (d, *J* = 3.0 Hz), 134.8, 138.3, 143.1, 149.0, 164.6, 163.0/165.5 (d, *J* = 247.7 Hz); ESI-HRMS *m/z* calcd for $C_{20}H_{13}ClFN_3O$: 366.08039 [M+H$^+$], found: 366.08042.

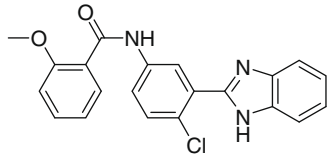

4.2.7. *N*-(3-(1*H*-Benzo[*d*]imidazol-2-yl)-4-chlorophenyl)-2-methoxybenzamide (12)

White solid, yield 84%. Mp = 181–182 °C; ^{1}H NMR (400 MHz, $(CD_3)_2SO$): δ = 3.89 (s, 3H), 7.06 (t, *J* = 7.6 Hz, 1H), 7.17 (d, *J* = 8 Hz, 1H), 7.23–7.24 (m, 2H), 7.48–7.52 (m, 1H), 7.59–7.64 (m, 4H), 7.90 (dd, *J* = 8.8 Hz, 2.4 Hz, 1H), 8.36 (d, *J* = 2.4 Hz, 1H), 10.39 (s, 1H), 12.72 (s, 1H); ^{13}C NMR (100 MHz, $(CD_3)_2SO$): δ = 55.9, 111.7, 112.0, 119.1, 120.4, 121.7, 122.1, 122.7, 124.7, 125.4, 129.6, 130.1, 130.5, 132.2, 138.2, 149.0, 156.5, 164.9, 170.3; ESI-HRMS *m/z* calcd for $C_{21}H_{16}ClN_3O_2$: 378.10038 [M+Na$^+$], found: 400.09233.

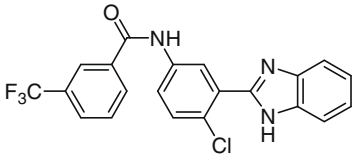

4.2.8. *N*-(3-(1*H*-Benzo[*d*]imidazol-2-yl)-4-chlorophenyl)-3-(trifluoromethyl)benzamide (13)

White solid, yield 57%. Mp = 223–224 °C; ^{1}H NMR (400 MHz, $(CD_3)_2SO$): δ = 7.22–7.26 (m, 2H), 7.59 (d, *J* = 7.2 Hz, 1H), 7.68 (d, *J* = 9.2 Hz, 1H), 7.70 (d, *J* = 7.2 Hz, 1H), 7.79 (t, *J* = 7.6 Hz, 1H), 7.97–8.03 (m, 2H), 8.29 (d, *J* = 7.6 Hz, 1H), 8.34 (s, 1H), 8.42 (d, *J* = 2.4 Hz, 1H), 10.74 (s, 1H); 12.71 (s, 1H); ^{13}C NMR (100 MHz, $(CD_3)_2SO$): δ = 111.9, 119.0, 121.8, 122.8, 123.6, 124.3, 125.8, 128.5, 129.4, 129.9, 130.0, 130.7, 132.0, 134.8, 135.3, 138.1, 143.1, 148.9, 164.2; ^{19}F NMR (376.4 MHz, $CDCl_3$): δ = −56.7 (s, 3F); ESI-HRMS *m/z* calcd for $C_{21}H_{13}ClF_3N_3O$: 416.07720 [M+H$^+$], found: 416.07756.

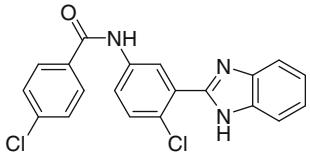

4.2.9. *N*-(3-(1*H*-Benzo[*d*]imidazol-2-yl)-4-chlorophenyl)-4-chlorobenzamide (14)

Yellow solid, yield 95%. Mp = 201–204 °C; ^{1}H NMR (200 MHz, $(CD_3)_2SO$): δ = 7.22–7.28 (m, 2H), 7.57–7.73 (m, 5H), 8.00–8.05 (m, 3H), 8.42 (d, *J* = 3.0 Hz, 1H), 10.59 (s, 1H), 12.70 (br, 1H); ^{13}C NMR (100 MHz, $(CD_3)_2SO$): δ = 111.8, 119.0, 121.8, 122.6, 122.8, 123.4, 125.6, 128.5, 129.7, 130.6, 133.1, 134.7, 136.7, 138.2, 143.1, 148.9, 164.6; ESI-HRMS *m/z* calcd for $C_{20}H_{13}Cl_2N_3O$: 382.05084 [M+H$^+$], found: 382.05058.

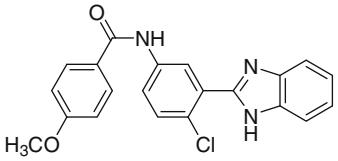

4.2.10. *N*-(3-(1*H*-Benzo[*d*]imidazol-2-yl)-4-chlorophenyl)-4-methoxybenzamide (15)

Orange solid, yield 88%. Mp = 188–191 °C; ^{1}H NMR (300 MHz, $(CD_3)_2SO$): δ = 3.99 (s, 3H), 7.06 (d, *J* = 8.7 Hz, 2H), 7.21–7.24 (m, 2H), 7.56–7.72 (m, 4H), 7.96–8.00 (m, 2H), 8.41 (d, *J* = 2.7 Hz, 1H), 10.37 (s, 1H), 12.67 (br, 1H); ^{13}C NMR (100 MHz, $(CD_3)_2SO$): δ = 55.5, 113.7, 114.1, 113.7, 122.6, 123.3, 125.2, 126.2, 129.7, 129.9, 130.5, 138.6, 142.2, 149.1, 162.2, 165.1; ESI-HRMS *m/z* calcd for $C_{21}H_{16}ClN_3O_2$: 378.10038 [M+H$^+$], found: 378.10033.

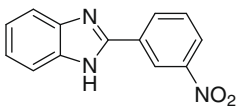

4.2.11. 2-(3-Nitrophenyl)-1*H*-benzo[*d*]imidazole (17)

To a stirred solution of diaminobenzene (1.26 g, 11.7 mmol) in THF (50 ml) triethyl amine (2.50 ml, 17.5 mmol) and 3-nitrobenzoyl chloride (2.27 g, 12.2 mmol) were added at 0 °C. The solution was stirred for 15 h at rt. The solvent was removed under reduced pressure and the crude intermediate product was purified by column chromatography (*n*-hexane/ethyl acetate 1:1 *v*/*v*) yielding the intermediate amide (1.29 g, 5.0 mmol) as a yellow solid. It was dissolved in acetic acid (45 ml) and refluxed for 2 h. After cooling down to rt the solution was poured on ice and extracted with dichloromethane (3 × 50 ml). The organic phases were dried over

sodium sulphate and **17** was obtained as a orange solid (1.21 g, 43%); mp = 184–187 °C; ^{1}H NMR (400 MHz, $(CD_3)_2SO$): δ = 7.15 (d, J = 7.2 Hz, 1H), 7.31–7.33 (m, 2H), 7.67–7.70 (m, 2H) 7.78–7.82 (m, 1H), 8.37–8.40 (m, 2H), 10.35 (br, 1H); ^{13}C NMR (75 MHz, $(CD_3)_2SO$): δ = 116.0, 116.1, 122.6, 125.9, 126.2, 130.0, 130.2, 134.3, 136.1, 147.7, 163.6; ESI-HRMS *m/z* calcd for $C_{13}H_9N_3O_2$: 240,07675 [M+H$^+$], found: 240.07677.

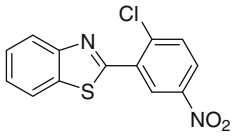

4.2.12. 2-(2-Chloro-5-nitrophenyl)benzo[*d*]thiazole (22)

A solution of 2-aminothiophenol **20** (1.0 ml, 9.27 mmol), 2-chloro-5-nitrobenzaldehyde **21** (1.72 g, 9.27 mmol) and iodine (1.18 g, 4.63 mmol) in DMF (2.5 ml) was stirred at rt for 15 h. The solvent was removed under reduced pressure. The crude product was purified by column chromatography (hexane/EtOAc 3:1 *v*/*v*) yielding **22** (2.0 g, 74%) as a yellow solid; mp = 106 °C; ^{1}H NMR (400 MHz, $(CD_3)_2SO$): δ = 6.83–6.85 (m, 1H), 6.94–6.98 (m, 1H), 7.01–7.03 (m, 1H), 7.16 (d, J = 3.2 Hz, 1H), 7.80 (d, J = 8.8 Hz, 1H), 8.16 (dd, J = 8.4 Hz, 2.8 Hz, 1H,), 8.31 (d, J = 3.2 Hz, 1H); ^{13}C NMR (100 MHz, $(CD_3)_2SO$): δ = 119.9, 121.4, 121.7, 123.5, 124.3, 126.0, 131.4, 137.3, 137.9, 143.1, 147.0, 151.6, 161.3; ESI-HRMS *m/z* calcd for $C_{13}H_8ClN_2O_2S$: 290.99950 [M+H$^+$], found: 290.99895.

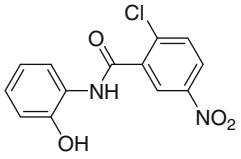

4.2.13. 2-Chloro-*N*-(2-hydroxyphenyl)-5-nitrobenzamide (27)

A solution of 2-aminophenol **25** (4.0 g, 19.8 mmol), 2-chloro-5-nitrobenzoyl chloride **26** (4.4 g, 19.8 mmol), and triethyl amine (3.98 ml, 28.4 mmol) in THF (8.0 ml) was stirred at rt for 15 h. The solvent was removed under reduced pressure. The crude product was purified by column chromatography (hexane/EtOAc 1:1, *v*/*v*) yielding **27** (5.09 g, 88%) as a yellow solid; mp = 190–192 °C; ^{1}H NMR (300 MHz, $(CD_3)_2SO$): δ = 6.80–6.85 (m, 1H), 6.90 (m, 1H), 7.00–7.06 (m, 1H), 7.79–7.84 (m, 2H), 8.29 (dd, J = 8.9 Hz, 2.6 Hz, 1H), 8.42 (d, J = 2.7 Hz, 1H), 9.78 (br, 1H), 9.93 (br, 1H); ^{13}C NMR (75 MHz, $(CD_3)_2SO$): δ = 115.8, 119.0, 123.8, 124.2, 125.2, 125.5, 125.9, 131.2, 137.3, 137.7, 146.0, 149.1, 163.2; ESI-HRMS *m/z* calcd for $C_{13}H_{10}ClN_2O_4$: 293.03291 [M+H$^+$], found: 293.03236.

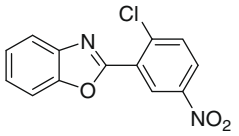

4.2.14. 2-(2-Chloro-5-nitrophenyl)benzo[*d*]oxazole (28)

A solution of 2-chloro-*N*-(2-hydroxyphenyl)-5-nitrobenzamide **27** (2.20 g, 7.52 mmol, see above) and *p*-toluenesulfonic acid monohydrate (3.06 g, 16.1 mmol) in *o*-xylole (75 ml) was refluxed for 4 h. After cooling down to rt the solution was diluted with EtOAc (70 ml), washed with $NaHCO_3$ (2 × 60 ml, half-concentrated) and the aqueous phase reextracted with EtOAc (30 ml). The combined organic phases were washed with brine (70 ml) and dried over sodium sulfate. The solvent was removed under reduced pressure. The crude product was purified by column chromatography (hexane/EtOAc 5:1 *v*/*v*) yielding **28** (2.06 g, 99%) as a yellow solid; mp = 170–172 °C; ^{1}H NMR (400 MHz, $(CD_3)_2SO$): δ = 7.45–7.54 (m, 2H), 7.85–7.91 (m, 2H), 7.99 (d, J = 8.8 Hz, 1H), 8.39 (dd, J = 8.8 Hz, 2.8 Hz, 1H), 8.87 (d, J = 2.8 Hz, 1H); ^{13}C NMR (100 MHz, $(CD_3)_2SO$): δ = 111.3, 120.5, 125.3, 126.3, 126.6, 126.8, 133.1, 138.7, 138.7, 140.9, 146.4, 150.0, 158.2; ESI-HRMS *m/z* calcd for $C_{13}H_8ClN_2O_3$: 275.02234 [M+H$^+$], found: 275.02180.

4.3. General procedure for preparing benzamines 18, 23, 29

The procedure is described for **18** (3-(1*H*-benzo[*d*]imidazol-2-yl)benzenamine). A suspension containing 2-(3-nitrophenyl)-1*H*-benzo[*d*]imidazole (1.15 g, 4.81 mmol), iron (0.81 g, 14.4 mmol) and concd HCl (2.0 ml) in ethanol (17 ml) was refluxed for 3 h. After cooling down to rt the mixture was diluted with EtOAc (30 ml) and washed with water (20 ml) and brine (20 ml). The organic phase was dried over Na_2SO_4. After removing the solvent under reduced pressure the crude product was chromatographed on silica gel to obtain **18** (758 mg, 75%) as a grey solid.

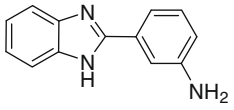

4.3.1. 3-(1*H*-Benzo[*d*]imidazol-2-yl)benzenamine (18)

Grey solid, yield 75%. Mp = 247–249 °C; ^{1}H NMR (200 MHz, $(CD_3)_2SO$): δ = 5.27 (br, 2H), 6.65 (d, J = 7.8 Hz, 1H), 7.10–7.28 (m, 4H), 7.40–7.46 (m, 2H), 7.59 (d, J = 8.2 Hz, 1H), 12.68 (br, 1H); ^{13}C NMR (50 MHz, $(CD_3)_2SO$): δ = 111.1, 111.9, 114.0, 115.5, 118.7, 121.4, 122.2, 129.3, 130.7, 134.9, 143.8, 149.1, 152.1; ESI-HRMS *m/z* calcd for $C_{13}H_{12}N_3$: 210.10312 [M+H$^+$], found: 210.10257.

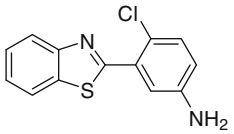

4.3.2. 3-(Benzo[*d*]thiazol-2-yl)-4-chlorobenzenamine (23)

Yellow solid, yield 57%. Mp = 118–120 °C; ^{1}H NMR (400 MHz, $(CD_3)_2SO$): δ = 5.55 (br, 2H), 6.75 (dd, J = 8.6 Hz, 2.6 Hz, 1H), 7.26 (d, J = 8.8 Hz, 1H), 7.45–7.49 (m, 2H), 7.53–7.57 (m, 1H), 8.07 (d, J = 8.4 Hz, 1H), 8.15 (d, J = 8.0 Hz, 1H); ^{13}C NMR (100 MHz, $(CD_3)_2SO$): δ = 115.6, 117.0, 117.5, 122.0, 122.9, 125.5, 126.5, 131.1, 131.3, 135.3, 148.2, 152.0, 164.2; ESI-HRMS *m/z* calcd for $C_{13}H_{10}ClN_2S$: 261.02532 [M+H$^+$], found: 261.02477.

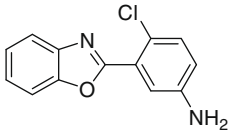

4.3.3. 3-(Benzo[*d*]oxazol-2-yl)-4-chlorobenzenamine (29)

Yellow solid, yield 96%. Mp = 138–139 °C; ^{1}H NMR (400 MHz, $(CD_3)_2SO$): δ = 5.62 (br, 2H), 6.78 (dd, J = 8.4 Hz, 2.8 Hz, 1H), 7.27 (d, J = 8.8 Hz, 1H), 7.35 (d, J = 2.8 Hz, 1H), 7.35–7.46 (m, 2H), 7.77 (dd, J = 7.0 Hz, 2.2 Hz, 1H), 7.83 (dd, J = 7.0 Hz, 2.5 Hz, 1H); ^{13}C NMR (100 MHz, $(CD_3)_2SO$): δ = 110.9, 115.9, 117.5, 118.0, 120.0,

124.8, 125.3, 125.7, 131.5, 141.1, 148.1, 149.9, 160.9; ESI-HRMS *m/z* calcd for $C_{13}H_{10}ClN_2O$: 245.04817 [M+H$^+$], found: 245.04762.

4.4. General procedure for preparing benzimidazoles 19, 24, 30

The procedure is described for *N*-(3-(1*H*-benzo[*d*]imidazol-2-yl)phenyl)-3,4,5-triethoxybenzamide **19**. A solution of 3-(1*H*-benzo[*d*]imidazol-2-yl)benzenamine **18** (280 mg, 1.34 mmol), 3,4,5-triethoxybenzoyl chloride (383 mg, 1.41 mmol, 1.05 equiv), DMAP (17 mg, 0.14 mmol) and triethyl amine (0.28 ml, 2.01 mmol) in dry THF (8.0 ml) was stirred at rt for 15 h. The solvent was removed under reduced pressure. The crude product was chromatographed on silica gel yielding **18** (474 mg, 79%) as a white solid.

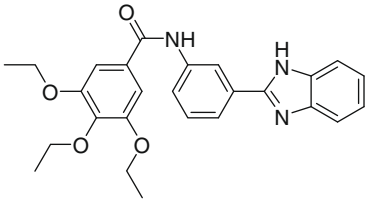

4.4.1. *N*-(3-(1*H*-Benzo[*d*]imidazol-2-yl)phenyl)-3,4,5-triethoxybenzamide (19)

White solid, yield 79%. Mp = 201–202 °C; ^{1}H NMR (200 MHz, $(CD_3)_2SO$): δ = 1.24 (t, *J* = 7.0 Hz, 3H), 1.35 (t, *J* = 6.9 Hz, 6H), 3.94–4.16 (m, 6H), 7.15–7.18 (m, 2H), 7.31 (s, 2H), 7.45–7.65 (m, 3H), 7.83–7.93 (m, 2H), 8.61 (s, 1H), 10.23 (br, 1H), 12.89 (br, 1H); ^{13}C NMR (50 MHz, $(CD_3)_2SO$): δ = 14.7, 15.4, 64.2, 68.0, 106.3, 111.3, 118.8, 119.0, 121.4, 121.6, 121.9, 122.4, 129.1, 129.3, 130.5, 135.0, 139.7, 140.0, 143.8, 151.1, 152.2, 164.8; ESI-HRMS *m/z* calcd for $C_{26}H_{28}N_3O_4$: 446.20798 [M+H$^+$], found: 446.20743.

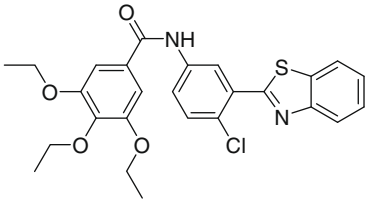

4.4.2. *N*-(3-(Benzo[*d*]thiazol-2-yl)-4-chlorophenyl)-3,4,5-triethoxybenzamide (24)

Yellow solid, yield 77%. Mp = 171–174 °C; ^{1}H NMR (300 MHz, $(CD_3)_2SO$): δ = 1.24 (t, *J* = 7.1 Hz, 3H), 1.35 (t, *J* = 6.9 Hz, 6H), 4.01 (q, *J* = 7.0 Hz, 2H), 4.11 (q, *J* = 7.0 Hz, 4H), 7.30 (s, 2H), 7.48–7.54 (m, 1H), 7.56–7.62 (m, 1H), 7.67 (d, *J* = 9.0 Hz, 1H), 8.06 (dd, *J* = 9.0 Hz, 2.7 Hz, 1H), 8.13 (d, *J* = 7.8 Hz, 1H), 8.18–8.21 (m, 1H), 8.68 (d, *J* = 2.4 Hz, 1H), 10.40 (br, 1H); ^{13}C NMR (75 MHz, $(CD_3)_2SO$): δ = 14.7, 15.4, 64.3, 68.0, 106.4, 122.2, 122.7, 123.0, 123.7, 125.4, 125.8, 126.8, 129.0, 131.2, 135.4, 138.7, 140.2, 151.8, 152.2, 163.2, 165.1; ESI-HRMS *m/z* calcd for $C_{26}H_{26}ClN_2O_4S$: 497.13018 [M+H$^+$], found: 497.12963.

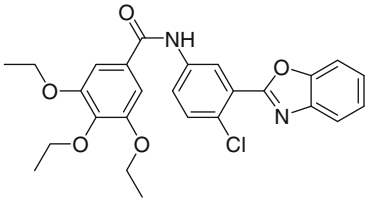

4.4.3. *N*-(3-(Benzo[*d*]oxazol-2-yl)-4-chlorophenyl)-3,4,5-triethoxybenzamide (30)

White solid, yield 82%. Mp = 191–193 °C; ^{1}H NMR (400 MHz, $CD_3)_2SO$): δ = 1.28 (t, *J* = 7.2 Hz, 3H), 1.39 (t, *J* = 6.8 Hz, 6H), 4.03 (q, *J* = 6.8 Hz, 2H), 4.14 (q, *J* = 6.9 Hz, 4H), 7.32 (s, 2H), 7.48–7.52 (m, 2H), 7.71 (d, *J* = 8.8 Hz, 1H), 8.08 (d, *J* = 2.8 Hz, 1H), 8.10 (d, *J* = 2.4 Hz, 1H), 8.69 (s, 1H), 10.43 (br, 1H); ^{13}C NMR (100 MHz, $CD_3)_2SO$): δ = 14.7, 15.4, 64.3, 68.1, 106.4, 111.0, 120.2, 122.9, 124.2, 125.1, 125.2, 126.1, 129.0, 131.7, 138.6, 140.2, 141.0, 150.0, 152.2, 160.0, 165.1; ESI-HRMS *m/z* calcd for $C_{26}H_{26}ClN_2O_5$: 481.15302 [M+H$^+$], found: 481.15248.

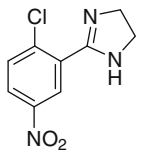

4.4.4. 2-(2-Chloro-5-nitrophenyl)-4,5-dihydro-1*H*-imidazole (32)

To a solution of 2-Chloro-5-nitrobenzaldehyde **21** (2.56 g, 13.78 mmol) in *t*-BuOH (138 ml) was added ethylendiamine (0.91 g, 15.16 mmol). The obtained mixture was stirred at rt under an argon atmosphere for 30 min, and then K_2CO_3 (5.71 g, 41.33 mmol) and iodine (4.37 g, 17.22 mmol) were added to the mixture and stirred at 70 °C. After 3 h, the mixture was quenched with satd Na_2SO_3 solution until iodine colour almost disappeared, and was extracted with $CHCl_3$ (3 × 150 ml). The organic layer was washed with satd $NaHCO_3$ solution and brine, and dried over Na_2SO_4. After filtration the mixture was evaporated in vacuo and purified by silica gel FC (MeOH/EtOAc 1:1 *v*/*v*) to give **32** (3.0 g, 99%) as an orange solid; mp = 123–124 °C; ^{1}H NMR (300 MHz, $CDCl_3$): δ = 3.80 (s, 4H), 5.10 (br, 1H), 7.55 (d, *J* = 9 Hz, 1H), 8.15 (dd, *J* = 8.7 Hz, 2.7 Hz, 1H), 8.56 (d, *J* = 2.7 Hz, 1H); ^{13}C NMR (50 MHz, $CDCl_3$): δ = 50.6, 125.5, 126.6, 131.6, 132.1, 139.0, 146.5, 161.7; ESI-HRMS *m/z* calcd for $C_9H_8ClN_3O_2$: 226.03778 [M+H$^+$], found: 226.03757.

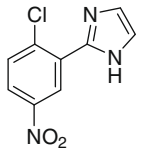

4.4.5. 2-(2-Chloro-5-nitrophenyl)-1*H*-imidazole (35)

To a mixture of 2-(2-Chloro-5-nitrophenyl)-4,5-dihydro-1*H*-imidazole **33** (0.82 g, 3.64 mmol) and K_2CO_3 (0.55 g, 4.0 mmol) in DMSO (36 ml) was added DIB (1.29 g, 4.0 mmol). Then the mixture was stirred for 3 days at rt under argon. Then, the reaction mixture was diluted with satd $NaHCO_3$ solution (20 ml) and EtOAc (15 ml), and was stirred for 5 min. After extraction with EtOAc (3 × 80 ml) the organic layer was dried over Na_2SO_4, concentrated and purified by FC (hexane/EtOAc 4:1–2:1 + 1% amine, *v*/*v*) to give **35** (0.54 g, 66%) as a yellow solid; mp = 170–172 °C; ^{1}H NMR (400 MHz, $CDCl_3$): δ = 7.27 (d, *J* = 10.8 Hz, 2H), 7.61 (d, *J* = 8.8 Hz, 1H), 8.11 (dd, *J* = 9.2 Hz, 2.8 Hz, 1H), 9.19 (d, *J* = 2.8 Hz, 1H), 10.37 (br, 1H); ^{13}C NMR (100 MHz, $CDCl_3$): δ = 123.5, 125.9, 127.3, 130.0, 131.8, 135.5, 141.9, 147.3; ESI-HRMS *m/z* calcd for $C_9H_6ClN_3O_2$: 224.022013 [M+H$^+$], found: 224.02201.

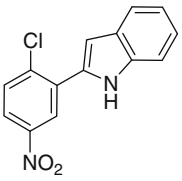

4.4.6. 2-(2-Chloro-5-nitrophenyl)-1*H*-indole (40)

2-Chloro-5-nitroacetophenone **39** (0.50 g, 2.51 mmol) and phenylhydrazine hydrochloride **38** (0.54 g, 3.758 mmol) were

mixed with EtOH (2.5 ml) and two drops of glacial AcOH and heated slowly to 80 °C and the mixture was stirred over night at this temperature. The solvent was evaporated to give a yellow solid. PPA (1.5 ml) was added and the mixture was slowly heated to 120 °C, stirred for 15 min and poured on ice and neutralised with 2 M NaOH (5 ml). The obtained precipitate was filtrated to give **40** (0.68 g, 100%) as a brown solid in an almost pure state; ^{1}H NMR (300 MHz, $(CD_3)_2SO$): δ = 7.05 (t, J = 7.4 Hz, 1H), 7.11 (d, J = 2.1 Hz, 1H), 7.18 (t, J = 7.4 Hz, 1H), 7.46 (d, J = 8.4 Hz, 1H), 7.62 (d, J = 8.1 Hz, 1H), 7.89 (d, J = 8.7 Hz, 1H), 8.17 (dd, J = 8.7 Hz, 2.7 Hz, 1H), 8.56 (d, J = 2.4 Hz, 1H), 11.74 (s, 1H); ^{13}C NMR (75 MHz, $(CD_3)_2SO$): δ = 104.7, 11.6, 119.7, 120.8, 122.8, 123.0, 124.5, 127.8, 131.9, 132.2, 136.7, 137.4, 146.6; ESI-HRMS *m/z* calcd for $C_{14}H_9ClN_2O_2$: 273.04253 [M+H$^+$], found: 273.04256.

4.5. General procedure for preparing benzamines 33, 36, 41

The procedure is described for **36**. A suspension containing 2-(2-chloro-5-nitrophenyl)-1*H*-imidazole **35** (142 mg, 0.64 mmol), iron (106 mg, 1.89 mmol) and concd HCl (0.27 ml) in ethanol (3 ml) was refluxed for 3 h. After cooling down to rt the mixture was diluted with EtOAc (9 ml) and washed with water (9 ml) and satd $NaHCO_3$ solution (9 ml). The aqueous layer was washed with EtOAc (3 × 9 ml) and the organic phase was dried over Na_2SO_4. After removing the solvent under reduced pressure the crude product was chromatographed on silica gel to obtain **36** (110 mg, 89%) as a yellow oil.

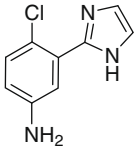

4.5.1. 4-Chloro-3-(1*H*-imidazol-2-yl)benzamine (36)

Yellow oil, yield 89%. ^{1}H NMR (300 MHz, $(CD_3)_2SO$): δ = 5.33 (s, 2H), 6.56 (dd, J = 8.4 Hz, 2.7 Hz, 1H), 6.96–7.17 (m, 4H), 12.03 (br, 1H); ^{13}C NMR (75 MHz, $(CD_3)_2SO$): δ = 115.3, 115.8, 116.4, 117.4, 123.5, 130.2, 143.6, 145.7, 147.7; ESI-HRMS *m/z* calcd for $C_9H_8ClN_3$: 194.04795 [M+H$^+$], found: 194.04806.

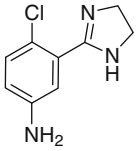

4.5.2. 4-Chloro-3-(4,5-dihydro-1*H*-imidazol-2-yl)benzamine (33)

Colourless oil, yield 50%. ^{1}H NMR (200 MHz, $(CD_3)_2SO$): δ = 3.13 (s, 4H), 5.30 (s, 2H), 6.54 (dd, J = 8.8 Hz, 2.6 Hz, 1H), 6.70 (d, J = 2.4 Hz, 1H), 7.02 (d, J = 8.8 Hz, 1H); ^{13}C NMR (100 MHz, $(CD_3)_2SO$): δ = 48.6, 115.4, 115.8, 116.8, 129.9, 131.7, 147.4, 163.4; ESI-HRMS *m/z* calcd for $C_9H_{10}ClN_3$: 196.06360 [M+H$^+$], found: 196.06353.

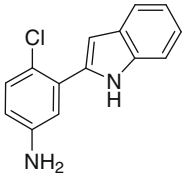

4.5.3. 4-Chloro-3-(1*H*-indol-2-yl)benzamine (41)

Yellow oil, yield 80%. ^{1}H NMR (300 MHz, $(CD_3)_2SO$): δ = 5.36 (s, 2H), 6.59 (dd, J = 8.7 Hz, 2.7 Hz, 1H), 6.70 (d, J = 2.1 Hz, 1H), 6.86 (d, J = 2.7 Hz, 1H), 7.00 (t, J = 7.5 Hz, 1H), 7.10 (t, J = 8.1 Hz, 1H), 7.18 (d, J = 8.7 Hz, 1H), 7.40 (d, J = 8.1 Hz, 1H), 7.55 (d, J = 7.5 Hz, 1H), 11.23 (s, 1H); ^{13}C NMR (100 MHz, $(CD_3)_2SO$): δ = 102.2, 11.3, 114.7, 115.5, 117.1, 119.1, 120.0, 121.4, 127.9, 130.6, 131.5, 135.4, 136.3, 147.8; ESI-HRMS *m/z* calcd for $C_{14}H_{11}ClN_2$: 243.06835 [M+H$^+$], found: 243.06815.

4.6. General procedure for preparing benzamides 34, 37, 42

The procedure is described for **37** (KS79). 3,4,5-triethoxybenzoic acid (139 mg, 0.55 mmol) was dissolved in dry CH_2Cl_2 (1 ml) and cooled to 0 °C under argon. Oxalylchloride (0.05 ml, 0.57 mmol) and two drops of DMF were added and the resulting mixture was stirred at 0 °C for 1.5 h and then 2 h at room temperature. The solvent was evaporated in vacuo to give a solid that was dried in vacuo. The crude acyl chloride (129 mg, 0.47 mmol, 0.95 equiv) was dissolved in CH_2Cl_2 (2 ml), and added drop wise into an ice-cooled solution of 4-chloro-3-(1*H*-imidazol-2-yl)benzamine (**36**) (96 mg, 0.50 mmol) and Et_3N (0.1 ml, 0.74 mmol) in anhydrous CH_2Cl_2 (2 ml). After stirring additional 15 min at 0 °C and at room temperature over night the solvent was removed under reduced pressure, and the residue was chromatographed on silica gel to obtain **37** as a yellow oil (36 mg, 18%).

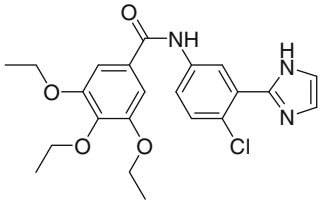

4.6.1. *N*-(4-Chloro-3-(1*H*-imidazol-2-yl)phenyl)-3,4,5-triethoxybenzamide (37)

Compound **37** was obtained as a yellow oil in 20% yield from 4-chloro-3-(1*H*-imidazol-2-yl)benzamine **36**. ^{1}H NMR (300 MHz, $(CD_3)_2SO$): δ = 1.24 (t, J = 7.2 Hz, 3H), 1.35 (t, J = 6.9 Hz, 6H), 4.00 (q, J = 7.2 Hz, 2H), 4.10 (q, J = 6.6 Hz, 4H), 7.06–7.25 (m, 4H), 7.51 (d, J = 8.7 Hz, 1H), 7.87 (dd, J = 8.7 Hz, 2.7 Hz, 1H), 8.18 (d, J = 2.7 Hz, 1H), 10.23 (s, 1H), 12.24 (br, 1H); ^{13}C NMR (50 MHz, $(CD_3)_2SO$): δ = 14.8, 15.5, 64.3, 68.1, 106.4, 107.5, 121.6, 122.8, 129.2, 130.3, 138.2, 142.8, 152.2, 165.0; ESI-HRMS *m/z* calcd for $C_{22}H_{24}ClN_3O_4$: 430.15281 [M+H$^+$], found: 430.15286.

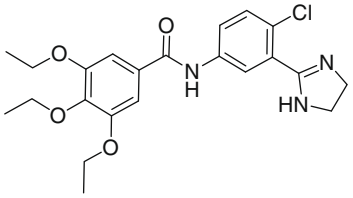

4.6.2. *N*-(4-Chloro-3-(4,5-dihydro-1*H*-imidazol-2-yl)phenyl)-3,4,5-triethoxybenzamide (34)

Yellow oil, yield 81%. ^{1}H NMR (400 MHz, $CD_3)_2SO$): δ = 1.15 (t, J = 7.1 Hz, 3H), 1.29 (t, J = 6.9 Hz, 6H), 3.80–3.98 (m, 10H), 6.33 (dd, J = 8.7 Hz, 2.7 Hz, 1H), 6.55 (d, J = 2.7 Hz, 1H), 6.57 (s, 2H), 6.69 (d, J = 8.7 Hz, 1H); ^{13}C NMR (75 MHz, $(CD_3)_2SO$): δ = 14.8, 15.4, 48.5, 52.9, 64.0, 67.6, 106.8, 115.7, 115.9, 116.5, 128.9, 129.7, 131.2, 138.7, 147.2, 151.3, 156.8, 167.3; ESI-HRMS *m/z* calcd for $C_{22}H_{26}ClN_3O_4$: 432.16846 [M+H$^+$], found: 432.16861.

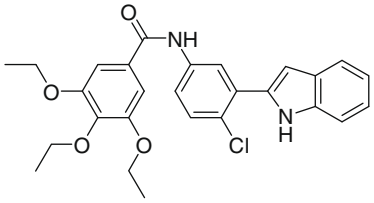

4.6.3. *N*-(4-Chloro-3-(1*H*-indol-2-yl)phenyl)-3,4,5-triethoxybenzamide (42)

Colourless oil, yield 90%. ^{1}H NMR (300 MHz, $(CD_3)_2SO$): δ = 1.24 (t, J = 7.2 Hz, 3H), 1.35 (t, J = 6.9 Hz, 6H), 4.01 (q, J = 7.2 Hz, 2H),

4.10 (q, J = 6.6 Hz, 4H), 6.81 (d, J = 1.5 Hz, 1H), 7.02 (t, J = 7.4 Hz, 1H), 7.12 (t, J = 7.4 Hz, 1H), 7.26 (s, 1H), 7.42 (d, J = 7.8 Hz, 1H), 7.55–7.59 (m, 2H), 7.76 (dd, J = 8.7 Hz, 2.4 H, 1H), 8.12 (d, J = 2.4 Hz, 1H); ^{13}C NMR (75 MHz, $(CD_3)_2SO$): δ = 14.8, 15.5, 64.3, 68.1, 102.9, 106.4, 111.5, 119.4, 120.3, 121.1, 121.9, 122.6, 125.4, 127.9, 129.3, 130.6, 131.5, 134.5, 136.6, 138.3, 140.1, 152.2, 165.0; ESI-HRMS m/z calcd for $C_{27}H_{27}ClN_2O_4$: 479.17321 [M+H$^+$], found: 479.17287.

References and notes

1. (a) Taipale, J.; Beachy, P. A. *Nature* **2001**, *411*, 349; (b) Ingham, P. W.; McMahon, A. P. *Gene Dev.* **2001**, *15*, 3059.
2. (a) Porter, J. A.; Young, K. E.; Beachy, P. A. *Science* **1996**, *274*, 255; (b) Porter, J. A.; Ekker, S. C.; Park, W. J.; von Kessler, D. P.; Young, K. E.; Chen, C. H.; Ma, Y.; Woods, A. S.; Cotter, R. J.; Koonin, E. V.; Beachy, P. A. *Cell* **1996**, *86*, 21; Mann, R. K.; Beachy, P. A. *Annu. Rev. Biochem.* **2004**, *73*, 891.
3. Aikin, R. A.; Ayers, K. L.; Therond, P. P. *EMBO Rep.* **2008**, *9*, 330.
4. (a) Huangfu, D.; Anderson, K. V. *Proc. Natl. Acad. Sci. U.S.A.* **2005**, *102*, 11325; (b) Rohatgi, R.; Milenkovic, L.; Scott, M. P. *Science* **2007**, *317*, 372.
5. Fukushima, N.; Walter, K. M.; Ueko, T.; Sato, N.; Matsubayashi, H.; Cameron, J. L.; Hruban, R. H.; Canto, M.; Yeo, C. J.; Goggins, M. *Cancer Biol. Ther.* **2003**, *2*, 78.
6. Karhadkar, S. S.; Bova, G. S.; Abdallah, N.; Dhara, S.; Gardner, D.; Maitra, A.; Isaacs, J. T.; Berman, D. M.; Beachy, P. A. *Nature* **2004**, *431*, 707.
7. Berman, D. M.; Karhadkar, S. S.; Maitra, A.; Montes De Oca, R.; Gerstenblith, M. R.; Briggs, K.; Parker, A. R.; Shimada, Y.; Eshleman, J. R.; Watkins, D. N.; Beachy, P. A. *Nature* **2003**, *425*, 846.
8. Corcoran, R. B.; Scott, M. P. *J. Neurooncol.* **2001**, *53*, 307.
9. Di Magliano, M. P.; Hebrok, M. *Nat. Rev. Cancer* **2003**, *3*, 903; Rubin, L. L.; de Sauvage, F. J. *Nat. Rev. Cancer* **2006**, *5*, 1026.
10. Cooper, M. K.; Porter, J. A.; Young, K. E.; Beachy, P. A. *Science* **1998**, *280*, 1603.
11. Jain Rishi, K.; Kelleher, J., III; Peukert, S.; Sun, Y. PCT Int. Appl., 2007; WO 2007120827 A2 20071025.
12. Williams, J. A.; Guicherit, O. M.; Zaharian, B. I.; Xu, Y.; Chai, L.; Wichterle, H.; Kon, C.; Gatchalian, C.; Porter, J. A.; Rubin, L. L.; Wang, F. Y. *Proc. Natl. Acad. Sci. U.S.A.* **2003**, *100*, 4616.
13. Chen, J. K.; Taipale, J.; Young, K. E.; Maiti, T.; Beachy, P. A. *Proc. Natl. Acad. Sci. U.S.A.* **2002**, *99*, 14071.
14. (a) Guicherit, O. M.; Boyd, E. A.; Brunton, S .A.; Price, S.; Stibbard, J. H. A.; MacKinnon, C. H. PCT Int. Appl., 2006; WO 2006050506 A1 20060511.; (b) Beachy, P. A.; Chen, J. K.; Taipale, A. J. N. PCT Int. Appl., 2003; WO 2003088970 A2 20031030.
15. Lee, J.; Wu, X.; Di Magliano, M. P.; Peters, E. C.; Wang, Y.; Hong, J.; Hebrok, M.; Ding, S.; Cho, C. Y.; Schultz, P. G. *ChemBioChem* **2007**, *8*, 1916.
16. Lauth, M.; Berström, A.; Shimokawa, T.; Toftgard, R. *Proc. Natl. Acad. Sci. U.S.A.* **2007**, *104*, 8455.
17. Wang, Y.; Zhouc, Z.; Walsh, C. T.; McMahon, A. P. *Proc. Natl. Acad. Sci. U.S.A.* **2009**, *106*, 2623.
18. (a) Ferrari, S.; Yanega, R. Effect of Cyclopamine on Medaka (Oryzias latipes) embryos. Course Experiment, Developmental Biology, Franklin&Marshall-College. 2000. http://www.swarthmore.edu/NatSci/sgilber1/DB_lab/Student/Medaka_cyclo.html.; (b) Loucks, E.; Schwend, T.; Ahlgren, S. *Birth Defects Research Part A: Clinical and Molecular Teratology*, **2007**.
19. Chiang, C.; Litingtung, Y.; Lee, E.; Young, K. E.; Corden, J. L.; Westphal, H.; Beachy, P. A. *Nature* **1996**, *383*, 407.
20. Gong, B.; Hong, F.; Kohm, C.; Bonham, L.; Klein, P. *Bioorg. Med. Chem. Lett.* **2004**, *14*, 1455.
21. (a) Keeler, R. F.; Binns, W. *Teratology* **1968**, *1*, 5; (b) Incardona, J.; Gaffield, W.; Kapur, R.; Roelink, H. *Development* **1998**, *125*, 3553.